Available online at www.sciencedirect.com
ScienceDirect
Journal of Chromatography A, xxx (2007) xxx–xxx
JOURNAL OF CHROMATOGRAPHY A
www.elsevier.com/locate/chroma

Combined supercritical fluid chromatographic methods for the characterization of octadecylsiloxane-bonded stationary phases

E. Lesellier [a,b,*], C. West [a,b]

[a] *Groupe de Chimie Analytique de Paris-Sud, EA 4041, IUT d'Orsay, 91400 Orsay, France*
[b] *ICOA, UFR Sciences, UMR 6005, BP 6759, rue de Chartres, 45 067 Orleans cedex 2, France*

Received 19 February 2007; received in revised form 14 March 2007; accepted 19 March 2007

Abstract

In this paper, we present a combination of a key-solute test based on retention and separation factors of large probe solutes (carotenoid pigments) and a quantitative structure–retention relationship analysis based on the retention factors of small probe solutes (aromatic compounds) to investigate the different chromatographic behavior of octadecylsiloxane-bonded stationary phases of all sorts: classical, protected against silanophilic interactions or not, containing polar groups (endcapping groups or embedded groups). Varied chemometric methods are used to enlighten the differences between the 27 phases tested. The results indicate that the two approaches chosen (carotenoid test and solvation parameter model) are complementary and provide precise information on the chromatographic behavior of ODS phases.

Keywords: Stationary phases; ODS; Polar-embedded; Hydrophilic endcapping

1. Introduction

The characterization of the properties of the stationary phases used in high-performance liquid chromatography (HPLC) has been, for a long while, an important research topic for numerous research teams, column manufacturers and users.

Several tests are operated in HPLC, through the injection of probe solutes in varying mobile phases and operating conditions. The direct study of retention factors or separation factors allows evaluating (i) the hydrophobicity of the phase, that is to say its ability to retain solutes on the basis of dispersive interactions, (ii) the shape selectivity or steric selectivity and (iii) the presence of polar interactions, mainly due to non-bonded silanol groups, called residual silanol groups.

Indeed, the structures of the octadecylsiloxane-bonded silica (ODS) phases are very varied and can lead to very diverse selectivities:

(1) types of silica base: A, B (high purity) or C (surface covered with Si–H groups), organic/inorganic hybrid silica, silica covered with a polymer layer
(2) pore diameter,
(3) surface area,
(4) functionality of the bonding (mono- or poly-functional),
(5) bonding density,
(6) end-capping treatment: nature of the end-capping reactant, hydrophilic end-capping,
(7) bonded chains with steric protection and bidentate bonding,
(8) horizontal polymerization of the bonded chains,
(9) embedded polar groups (amide, urea, carbamate, quaternary ammonium, ether or sulphonamide).

The majority of these processes are intended to produce "base-deactivated" packings, that is to say to reduce the interactions of basic solutes with residual silanol groups. This can be done either by reducing the number of these silanol groups, or by reducing the access to these silanol groups, or by increasing the temperature and pH range resistance of the silica. The latter is to prevent silica's hydrolysis and allow its use in a pH were unwanted ionic interactions are unlikely (either at a low pH, because both basic solutes and silanol groups are protonated, or at a high pH because basic

* Corresponding author at: ICOA, UFR Sciences, UMR 6005, BP 6759, rue de Chartres, 45 067 Orleans cedex 2, France. Tel.: +33 1 69336131; fax: +33 1 69336048.
E-mail address: eric.lesellier@univ-orleans.fr (E. Lesellier).

0021-9673/$ – see front matter © 2007 Elsevier B.V. All rights reserved.
doi:10.1016/j.chroma.2007.03.072

solutes are not protonated and silanol groups are fully ionized).

The columns and their potentially very different selectivity require a classification in order to facilitate the selection of appropriate stationary phases for a given application. However, there is still no method that is generally accepted for this purpose.

The experimental results issued from chromatographic tests represent an impressive quantity, but the conclusions drawn from these results can be disappointing, either because the discrimination obtained is limited to large classes (C8/C18, classical/polar embedded phases), or because the presentation of the classification obtained is too complex. Moreover, the analytical conditions are often very different from one test to another. In particular, the pH and the proportion of organic solvent in the mobile phase can vary greatly, inducing little correlation between the factors supposedly evaluating the same properties [1,2]. In the same manner, the solutes chosen to evaluate a particular property are diverse and the conclusions can vary depending on the selected solutes.

Additionally, the different data treatment and modes of representation of the results can lead to different conclusions. In a previous paper, we have discussed numerical and graphical tools for the comparison of stationary phases and their relevance to the chromatographic reality [3]. In this paper, we had evidenced how the loss of information consecutive to improper data treatment and representations can induce misleading conclusions.

In contrast to the empirical testing procedures using arbitrary selected probes, quantitative structure–retention relationships (QSRRs) provide results that are independent of the solute set chosen, as long as the choice of solutes respects the requirements of diversity and independence of a good QSRR analysis. This approach allows describing the independent contribution of individual molecular interactions to the retention process. One of the most widely used QSRR is the so-called solvation parameter model, using Abraham's parameters [4,5]. Through this relationship, the retention of a compound can be related to specific interactions with the chromatographic system by the following equation:

$$\log k = c + eE + sS + aA + bB + vV \quad (1)$$

In Eq. (1), capital letters represent the solute descriptors, related to its particular interaction properties, while lower case letters represent the system constants, related to the complementary effect of the stationary and mobile phases on these interactions. c is the regression intercept, which is dominated by the phase ratio when the retention factor is used as the dependent variable. It also contains contributions from all sources of lack-of-fit of the model equation to the experimental retention data. E is the excess molar refraction (calculated from the refractive index of the molecule) and models polarizability contributions from n and π electrons; S is the solute dipolarity/polarizability; A and B are the solute overall hydrogen-bond acidity and basicity; V is the McGowan characteristic volume in units of $cm^3\ mol^{-1}/100$. The system constants (e, s, a, b, v), obtained through a multilinear regression of the retention data for a certain number of solutes with known descriptors (E, S, A, B, V), reflect the magnitude of difference for that particular property between the stationary and mobile phases. Thus, if a particular coefficient is numerically large, then any solute having the complementary property will interact very strongly with either the mobile phase (if the coefficient is negative) or the stationary phase (if the coefficient is positive). Consequently, the coefficients also reflect the system's relative selectivity towards that particular molecular interaction.

This approach has been used to characterize alkylsiloxane-bonded silica stationary phases in reversed-phase HPLC (RPLC) [6–12], but, in this case, the presence of water in the mobile phase partly conceals the subtle differences between the stationary phases. As a matter of fact, whatever the stationary phase, ODS, porous graphitic carbon (PGC) [13], fluorinated or cyano [14], the major terms in the equation are always the same: a positive v coefficient, indicating a high cavity energy in the highly cohesive aqueous mobile phase, and a negative b coefficient due to the strongly acidic water.

Eq. (1) has also been used in sub- or supercritical fluid chromatography (SFC) [15–22], on varied types of stationary phases. The results obtained allow a clear discrimination of all types of stationary phases, polar (bare silica, amino and cyano), non-polar (C4, C8 and different types of ODS), fluorinated (fluoroalkyl, fluorophenyl) or aromatic (PGC, propylphenyl, hexylphenyl, pyrenyl, etc). Indeed, when water is not present in the mobile phase, the slight differences between the stationary phases can be more thoroughly evaluated and Abraham's model is a powerful tool to achieve this task.

Besides, a test based on the analysis of carotenoid pigments was developed in SFC [23–25]. This test uses two separation factors and one retention factor of carotenoid pigments, measured in identical subcritical conditions (CO_2–methanol, 85:15, v/v), to compare the stationary phases.

Several types of structures are discriminated: polyfunctional phases (several C18 chains on one silanol group) with small pore diameter (100 Å), polyfunctional with large pore diameter (300 Å), polymer-coated silica, and four groups of monofunctional phases (one C18 chain per silanol group) with high or low bonding density, and with high or low protection against silanophilic interactions. Inside each group of monofunctional phases, the hydrophobicity criterion allows a finer comparison of the chromatographic behavior [24].

Polar-embedded ODS phases and phases with hydrophilic end-capping groups were also studied through this test [25]. The results agree well with the general knowledge that chromatographers have on these phases. These two types of phases sometimes have very close properties, but polar-endcapped phases are more retentive than the polar-embedded ones.

However, these phases were not clearly discriminated from classical monofunctional non-endcapped phases. Besides, some polar embedded groups can be discriminated (amide from carbamate, for instance) but some cannot (as sulphonamide from amide).

In this paper, the former classification (based on the carotenoid test) is completed and perfected by the use of the solvation parameter model and principal component analysis,

Please cite this article in press as: E. Lesellier, C. West, J. Chromatogr. A (2007), doi:10.1016/j.chroma.2007.03.072

based on the retention of 29 test-solutes in a subcritical carbon dioxide-methanol mobile phase.

The purpose of this study is to clearly discriminate the "polar ODS" phases by a precise characterization of the interactions they establish with the solutes.

2. Experimental

2.1. Stationary phases

All the stationary phases used in this study are commercially available and were kindly offered by the manufacturers. The names and known properties of the columns used are listed in Table 1. Unfortunately, not all manufacturers are willing to divulge the functionality, bonding technology and composition of their commercially available stationary phase column chemistries.

The columns were chosen for their representativeness of the possible treatments and bonding modes present in modern ODS phases.

2.2. Chemicals

Solvent used was HPLC grade methanol (MeOH) provided by Carlo Erba (Milan, Italy). Carbon dioxide was provided by l'Air Liquide (Paris, France).

β-Carotene isomers were obtained by iodine isomerization [26].

Twenty-nine aromatic compounds (see Table 2) were obtained from a range of suppliers. All the selected solutes are commercially available, not too expensive and stable enough to allow a long storage of their solutions. Solutions of these compounds were prepared in MeOH.

The solute descriptors used in the solvation parameter model were extracted from an in-house database established from several sources and are summarized in Table 2. The series of test compounds has been selected by observing the requirements of a good QSRR analysis. A minimum of four compounds per descriptor is generally recommended. We chose to work with a small set of compounds, knowing that the precision of the results is lesser than when larger sets of solutes are used. However, the compounds were chosen so as to provide a uniform distribution of each descriptor within a wide enough space and absence of cross-correlation among the descriptors was checked, indicating that the descriptors are close to orthogonality. Only slight correlations were observed between the descriptors. *E* and *S* present a little correlation but this was not unexpected as both *E* and *S* reflect the polarizability characteristics of the solute and no aliphatic solutes are present to break the covariance. *S* and *B* are also slightly dependent because they are similarly influenced by the presence of heteroatoms, inducing both higher H-bond basicity character (*B*) and a greater heterogeneity of the charge repartition among the structure of the solute (*S*). Similarly, *A* and *B* are slightly dependent because an acidic function is necessarily associated to the presence of a heteroatom, leading to an increased basic character. However, the choice of solutes is acceptable as the correlation coefficient is always inferior

Table 1
Stationary phases characterized is this study

Column	*n*	Manufacturer	Type of bonding
Uptisphere NEC	1	Interchim	Non-endcapped
Nucleosil 50 C18	2	Macherey-Nagel	Non-endcapped
Nucleosil 100 C18	3	Macherey-Nagel	Non-endcapped
Platinum EPS	4	Alltech-Grace	Unknown, low coverage bonding
Aquasil C18	5	Thermo Electron	Hydrophilic endcapping
Prevail C18	6	Alltech-Grace	Hydrophilic endcapping
Polaris C18-Ether	7	Metachem-Varian	Ether embedded
Polaris C18-B	8	Metachem-Varian	Unknown, possibly polar-embedded
Symmetry Shield	9	Waters	Carbamate embedded
Suplex pK_b	10	Supelco–Sigma	Urea embedded, non-endcapped
Supelcosil LC–ABZ	11	Supelco–Sigma	Amide embedded, endcapped
Supelcosil ABZ$^+$-Plus	12	Supelco–Sigma	Amide embedded, endcapped
Nucleosil Nautilus	13	Macherey-Nagel	Unknown, possibly amide embedded
Zorbax Bonus RP	14	Zorbax-Agilent	Amide embedded, sterically protected, endcapped
Acclaim PA	15	Dionex	Sulphonamide + ether embedded
Prevail amide	16	Alltech-Grace	Amide embedded
Stability BS C23	17	Cluzeau	Ammonium embedded
Zorbax StableBond	18	Zorbax-Agilent	Sterically protected chemistry, non-endcapped
Zorbax Eclipse XDB	19	Zorbax-Agilent	Double endcapping
XTerra MS C18	20	Waters	Hybrid inorganic/organic silica
Uptisphere ODB	21	Interchim	Endcapped
Chromolith C18 RPe	22	Merck	Monolith endcapped
Kromasil C18	23	Eka-Nobel	Endcapped
Zorbax Rx	24	Zorbax-Agilent	Dimethyloctadecylsilane, non-endcapped
Zorbax Extend	25	Zorbax-Agilent	Bidentate silane and double endcapping
Nucleosil AB	26	Macherey-Nagel	Polyfunctional
Gammabond	27	ES Industries	Polymer-coated alumina

Please cite this article in press as: E. Lesellier, C. West, J. Chromatogr. A (2007), doi:10.1016/j.chroma.2007.03.072

Table 2
Chromatographic solutes and LSER descriptors

n	Composé	*E*	*S*	*A*	*B*	*V*
1	Benzene	0.610	0.52	0.00	0.14	0.7164
2	Toluene	0.601	0.52	0.00	0.14	0.8573
3	Ethylbenzene	0.613	0.51	0.00	0.15	0.9982
4	Propylbenzene	0.604	0.50	0.00	0.15	1.1391
5	Butylbenzene	0.600	0.51	0.00	0.15	1.2800
6	Pentylbenzene	0.594	0.51	0.00	0.15	1.4209
7	Allylbenzene	0.717	0.60	0.00	0.22	1.0961
8	Anisole	0.708	0.75	0.00	0.29	0.9160
9	Methyl benzoate	0.733	0.85	0.00	0.48	1.0726
10	Benzaldehyde	0.820	1.00	0.00	0.39	0.8730
11	Acetophenone	0.818	1.01	0.00	0.48	1.0139
12	Benzonitrile	0.742	1.11	0.00	0.33	0.8711
13	Nitrobenzene	0.871	1.11	0.00	0.28	0.8906
14	Chlorobenzene	0.718	0.65	0.00	0.07	0.8288
15	Bromobenzene	0.882	0.73	0.00	0.09	0.8910
16	Naphtalene	1.340	0.92	0.00	0.20	1.0854
17	Biphenyl	1.360	0.99	0.00	0.26	1.3242
18	1-Phenylethanol	0.784	0.83	0.30	0.66	1.0570
19	Benzyl alcohol	0.803	0.87	0.39	0.56	0.9160
20	*o*-Cresol	0.840	0.86	0.52	0.46	0.9160
21	*m*-Cresol	0.822	0.88	0.57	0.34	0.9160
22	*p*-Cresol	0.820	0.87	0.57	0.31	0.9160
23	Phenol	0.805	0.89	0.60	0.30	0.7751
24	Resorcinol	0.980	1.00	1.10	0.58	0.8340
25	Phloroglucinol	1.355	1.12	1.40	0.82	0.8925
26	Benzoic acid	0.730	0.90	0.59	0.40	0.9317
27	Isophthalic acid	0.940	1.46	1.14	0.77	1.1470
28	Aniline	0.955	0.94	0.26	0.50	0.8162
29	*N*,*N*-Dimethylaniline	0.957	0.84	0.00	0.47	1.0980

E, excess molar refraction; *S*, dipolarity/polarizability; *A*, hydrogen bond acidity; *B*, hydrogen bond basicity; V, McGowan's characteristic volume.

to 0.70. We had previously characterized Kromasil C18 (column no.23) and Supelcosil ABZ$^+$-Plus (column no.12) with a larger set of solutes [20]; the results obtained with the larger set and the smaller set used here are not significantly different, at the 95% confidence level. Therefore, we consider this small set as perfectly valid and representative of the possible interactions occurring between the solutes and the chromatographic systems.

2.3. Chromatographic system and conditions

The chromatographic system used was described elsewhere [18] as well as the carotenoid test [23–25].

The carotenoid test is performed using carbon dioxide with 15% (v/v) MeOH.

The 29 test-compounds were chromatographed using carbon dioxide with 10% (v/v) MeOH as the smaller probes require a little less eluting mobile phase for precise measurement of retention factors.

For both tests, total flow through the system was 3.0 mL min^{-1}. Since the purpose of the present study is to investigate the effect of the nature of the stationary phase, all experiments were performed at constant outlet pressure and temperature. Column temperature was maintained at 25 °C. Back pressure was maintained at 150 bar. Inlet pressure varied among the different stationary phases between 175 and 185 bar.

In these conditions, the fluid is in its subcritical state. However, we have to point out that, to the chromatographer, the supercritical or subcritical state of the fluid is generally of no importance as most users of SFC do actually work in subcritical conditions without being aware of it. Indeed, the properties of the fluid face a continuous transition between the two phases. Besides, we believe that this distinction does nothing but maintain the confusion about SFC. Thus, whatever the real state of matter, subcritical or supercritical, we would tend to favor the use of "supercritical" when dealing with this form of chromatography and will therefore only use this term in the following.

UV-visible detection was carried out at 440 nm for carotenoid pigments and 254 nm for aromatic compounds.

Chromatograms were recorded using the AZUR software from Datalys (Surzur, France).

2.4. Data analysis

The logarithms of retention factors k of members of the homologous series vary linearly with the number of methylene groups. Therefore, the methylene selectivity α_{CH2} was obtained by calculating the slope of this relationship:

$$\log k_n = n \times \log \alpha_{CH2} + \log \rho \quad (2)$$

Where $\log k_n$ is the retention factor of a benzene–alkane, n is the number of carbon atoms in the alkyl chain (varied from 2 to 5)

Table 3
LSER models

Column	n	c	e	s	a	b	v	n	R^2_{adj}	SE	F
Uptisphere NEC	1	−0.819	0.598	−0.548			0.400	24	0.937	0.038	115.9
Nucleosil 50 C18	2	−0.830	0.551	−0.352			0.319	25	0.916	0.035	92.3
Nucleosil 100 C18	3	−0.882	0.528	−0.396			0.320	25	0.945	0.028	137.8
Platinum EPS	4	−1.327	0.351		0.471		0.292	24	0.938	0.062	122.3
Aquasil C18	5	−0.944	0.462	−0.190	0.284		0.305	26	0.949	0.037	121.4
Prevail C18	6	−0.827	0.536	−0.350	0.203		0.317	26	0.913	0.042	69.5
Polaris C18-Ether	7	−1.112	0.626	−0.504	0.203		0.328	28	0.903	0.047	66.4
Polaris C18-B	8	−1.193	0.451	−0.209	0.346	−0.469	0.448	27	0.920	0.039	60.5
Symmetry Shield	9	−0.849	0.606	−0.220	0.718	−0.384	0.179	27	0.979	0.041	248.1
Suplex pK_b	10	−1.096	0.673	−0.293	1.205	−0.370	0.200	24	0.976	0.054	186.8
Supelcosil LC–ABZ	11	−1.187	0.613	−0.199	1.215	−0.261	0.246	25	0.991	0.046	517.4
Supelcosil ABZ$^+$-Plus	12	−1.219	0.726	−0.305	1.348	−0.326	0.286	27	0.984	0.068	327.8
Nucleosil Nautilus	13	−1.008	0.433		1.018	−0.373	0.359	25	0.994	0.030	938.8
Zorbax Bonus RP	14	−1.106	0.317		0.867	−0.294	0.334	26	0.968	0.055	200.4
Acclaim PA	15	−0.816	0.542		0.446	−0.461	0.224	27	0.968	0.039	164.4
Prevail amide	16	−0.951	0.440		1.083			25	0.985	0.057	781.0
Stability BS C23	17	−1.245	0.576		1.702			23	0.965	0.100	322.5
Zorbax StableBond	18	−0.900	0.488	−0.437	−0.353	−0.163	0.406	25	0.964	0.036	131.3
Zorbax Eclipse XDB	19	−1.015	0.476	−0.347	−0.237	−0.367	0.518	29	0.922	0.064	67.5
XTerra MS C18	20	−1.115	0.358	−0.249	−0.379	−0.292	0.467	29	0.932	0.065	77.4
Uptisphere ODB	21	−0.801	0.559	−0.475	−0.284	−0.287	0.426	25	0.976	0.031	193.7
Chromolith C18 RPe	22	−1.197	0.508	−0.411	−0.367	−0.348	0.383	27	0.965	0.045	145.5
Kromasil C18	23	−0.888	0.428	−0.307	−0.469	−0.414	0.530	29	0.959	0.063	131.1
Zorbax Rx	24	−0.896	0.578	−0.486	−0.460	−0.352	0.377	27	0.980	0.040	250.5
Zorbax Extend	25	−0.895	0.516	−0.420	−0.493	−0.453	0.430	26	0.972	0.050	176.4
Nucleosil AB	26	−1.050	0.591	−0.406	−0.322	−0.444	0.420	27	0.932	0.071	71.8
Gammabond	27	−0.694	0.717	−0.630	−0.128	−0.262	0.314	27	0.938	0.047	79.7

n is the number of solutes considered in the regression, R^2_{adj} is the adjusted correlation coefficient, SE is the standard error in the estimate, *F* is the Fischer's statistic.

and log ρ represents the specific interaction of the residue of the molecule isolated from the alkyl chain.

The LSER system constants for each chromatographic system were obtained by multiple linear regression analysis for the logarithms of the measured retention factors. Multiple linear regression analysis and statistical tests were performed using the program SuperANOVA (Abacus Concept). The quality of the fits was estimated using the adjusted determination coefficient (R^2_{adj}), standard error in the estimate (SE) and Fischer *F* statistic. Descriptors that were not statistically significant, with a confidence interval of 95%, were eliminated from the model: from the Fischer (*F*) test, the relationship between the parameters and the dependent variable is expressed in terms of a probability (*p*) with a confidence interval of 95%. Thus, *p* should be lower than 0.05 to retain the tested parameter in the final equation. The system constants and statistics are summarized in Table 3.

The fits were all of reasonable quality, R^2_{adj} ranging from 0.903 to 0.995, standard error of estimate varying from 0.027 to 0.100. We consider these results as reasonably good. Naturally, in addition to goodness of fit, the coefficients must make chemical sense. The coefficients have been examined and are consistent with the known behavior of the stationary phases under study.

A few outliers were eliminated from the set as their residuals were too high. In any case, we verified that the test compounds retained in the model always still provided a wide and uniform distribution on each descriptor space, so that no bias was introduced by the elimination of outliers. In all cases, sufficient solutes were included in the model to give statistically meaningful model results. The number of solutes used in each model is provided in Table 3.

In most cases, the compounds needing to be excluded were of varied nature and no systematic trend was observed. However, for six columns (Uptisphere NEC no.1, Nucleosil 50 no.2, Nucleosil 100 no.3, Platinum EPS no.4, Aquasil no.5 and Prevail no.6), solutes no.28 (aniline) and 29 (*N*,*N*-dimethylaniline) had to be removed as they were extreme outliers and were largely more retained than what would be expected, based on the model calculations. These are the only *N*-containing bases in the solute set. Since oxygen-containing compounds of similar capacity for H-bond and dipole-type interactions (1-phenylethanol no.18 and benzyl alcohol no.19, for instance) are not influenced to the same extent, we presume that this additional retention results from a contribution to retention that is not considered by the model such as electrostatic interactions with residual silanol groups (in the non-end-capped phases) or other possibly ionized groups (in hydrophilic end-capped phases). Indeed, the solvation parameter model – in the form employed here – uses descriptors characteristic of the neutral form of the molecule. It is not expected to provide accurate predictions of chromatographic properties of solutes in a fully or partially ionized form. Different authors have suggested additional terms for ionizable solutes [27–32] but these descriptors require knowledge of the pH and pK_a of the species, while the pH of the carbon dioxide–methanol mobile phase is unknown. However, some studies tend to indicate that it could be acidic [33–35], possibly below 5, so aniline and *N*,*N*-

Please cite this article in press as: E. Lesellier, C. West, J. Chromatogr. A (2007), doi:10.1016/j.chroma.2007.03.072

dimethylaniline could be in their cationic (anilinium) form while the more acidic silanol groups could be in their anionic form. As no more precise information is available, we have to admit that electrostatic interactions occur but that we can so far not evaluate them.

In the same manner, for Stability BS C23 (no.17), benzoic acid (solute no.26) and isophthalic acid (no.27) had to be removed as they were extreme outliers. Electrostatic interactions must be assumed between the anionic forms of the acids and the quaternary ammonium embedded in the stationary phase. Besides, for this column, the results for the model fit are not as good as for the others (SE is the largest of all), indicating that the model may not be perfectly adapted to this phase.

In a previous paper [3], the applicability of the solvation vectors proposed by Ishihama and Asakawa [36] to the comparison of chromatographic systems was evidenced. Here, we chose to apply the same method with the five criteria issued from the solvation parameter model and, later, to the eight criteria issued from both the solvation parameter model and the carotenoid test. For the data issued from the carotenoid test, the logarithms of the retention and separation factors for carotenoid pigments were used, in order to have comparable values with the solvation parameter model coefficients.

The angle between two solvation vectors (ω) associated to two chromatographic systems can be calculated according to the following equation, based on the LSER coefficients of the two systems noted i and j:

$$\cos\,\theta_{ij} = \frac{\vec{\omega}_i \times \vec{\omega}_j}{|\vec{\omega}_i| \times |\vec{\omega}_j|}$$

Thus, when only the solvation parameter model coefficients are considered:

$$\cos\,\theta_{ij} = \frac{e_i e_j + s_i s_j + a_i a_j + b_i b_j + v_i v_j}{\sqrt{e_i^2 + s_i^2 + a_i^2 + b_i^2 + v_i^2}\sqrt{e_j^2 + s_j^2 + a_j^2 + b_j^2 + v_j^2}} \quad (3a)$$

And, when the solvation parameter model and the carotenoid tests are considered together:

$$\cos\,\theta_{ij} = \frac{e_i e_j + s_i s_j + a_i a_j + b_i b_j + v_i v_j + \beta_i \beta_j + \beta/zea_i * \beta/zea_j + c/t_i * c/t_j}{\sqrt{e_i^2 + s_i^2 + a_i^2 + b_i^2 + v_i^2 + \beta_i^2 + \beta/zea_i^2 + c/t_i^2}\sqrt{e_j^2 + s_j^2 + a_j^2 + b_j^2 + v_j^2 + \beta_j^2 + \beta/zea_j^2 + c/t_j^2}} \quad (3b)$$

where β is the logarithm of the retention factor of β-carotene; β/zea is the logarithm of the separation factor between β-carotene and zeaxanthin; c/t is the logarithm of the retention factor between 13-*cis*- and *all-trans*-β-carotene.

Furthermore, the similarity between two chromatographic systems is evaluated through the calculation of the J similarity factor, determined through Eqs. (4)–(6):

$$J = \cos\,\theta_{ij} - \cos\,(\theta_{di} + \theta_{dj}) \quad (4)$$

$$\cos(\theta_{di} + \theta_{dj}) = \sqrt{\left(1 - \frac{D_i^2}{|\vec{\omega}_i|^2}\right)\left(1 - \frac{D_j^2}{|\vec{\omega}_j|^2}\right)} - \frac{D_i D_j}{|\vec{\omega}_i|\vec{\omega}_j|} \quad (5)$$

$$D = \mathrm{TINV}(1 - 0.99, N) \times \mathrm{SE} \quad (6)$$

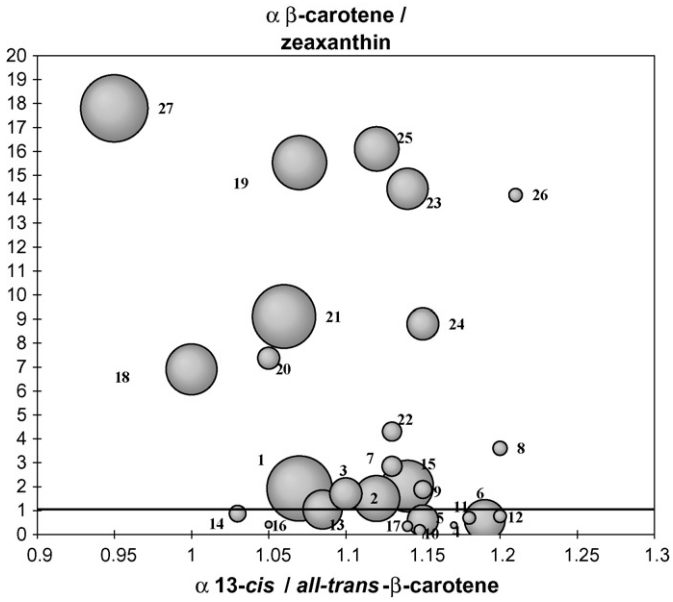

Fig. 1. Classification based on the carotenoid test. The separation factor between *all-trans*-β-carotene and zeaxanthin (silanophilic interaction) is plotted against the separation factor between the 13-*cis* and *all-trans* isomers of β-carotene (steric selectivity). The size of the bubbles is related to the retention factor of *all-trans*-β-carotene (hydrophobicity). Chromatographic conditions: CO_2–MeOH 85:15 (v/v), 3 mL min^{-1}, outlet pressure 150 bar, temperature 25 °C. The numbers indicate the columns as numbered in Table 1.

where TINV is the inverse of the Student's t-distribution for the specified degrees of freedom N, and SE is the average of the standard errors of the eight criteria.

In Eq. (4), when J is positive, the systems compared are found to be similar; in the opposite case, they are considered to be different.

Principal component analysis was performed with XLSTAT software (Microsoft Excel add-in for data analysis).

3. Results and discussion

3.1. Carotenoid test

Fig. 1 represents a classification diagram based on the carotenoid test. The separation factor between *all-trans*-β-carotene and *all-trans*-zeaxanthin is plotted against the separation factor between the 13-*cis* and the *all-trans* isomers of β-carotene. The size of the bubble is related to the retention factor of *all-trans*-β-carotene.

As previously described [23–25], a large value of the separation factor between *all-trans*-β-carotene and zeaxanthin indicates a low accessibility to residual silanol groups. The

comparison of the stationary phases being done with the same analytical conditions, the differences observed are only due to the differences in the solute–stationary phase interactions. Similarly to the caffeine–phenol separation [37], or to amiltryptiline/acenaphtene [38–40], the presence of residual silanol groups induces an increase in the retention of zeaxanthin that possesses two more hydroxyl groups, compared to β-carotene.

In Fig. 1, Gammabond C18 (no.27), Zorbax Eclipse XDB (no.19), Kromasil C18 (no.23), Zorbax Extend (no.25) and Nucleosil AB (no.26) are all well protected against silanophilic interactions. These results show that different treatments and bonding modes can lead to a similar chromatographic behavior as, among these columns are a bonded–coated–polymer column (Gammabond C18), a bidentate bonding with a propylene bridge (Zorbax Extend), a polyfunctional phase with a post-silanization treatment (Nucleosil AB), and two endcapped phases (Kromasil C18 and Zorbax Eclipse XDB).

A little less protected but still providing low accessibility to residual silanol groups, are Zorbax SB (no.18), XTerra MS (no.20), Uptisphere ODB (no.21) and Zorbax Rx (no.24). There again, the bonding chemistry or the nature of the silica can be very different, as XTerra MS is a hybrid organic–inorganic silica, Zorbax SB is a sterically protected phase and Uptisphere ODB is end-capped.

A finer discrimination of these phases can be made if one considers the separation factor between the two major isomers of β-carotene, the 13-*cis* and the *all-trans*. Indeed, former studies have shown that the separation of these bent and linear isomers depends on the structure of the stationary phase. The *cis/trans* separation of β-carotene describes the steric or shape selectivity of the stationary phase. For monofunctional phases, it increases in function of the bonding density between 1 and 1.2, and reaches its maximal values for polyfunctional phases. Thus, columns 18–25 are all monofunctional with an increasing bonding density from left to right on Fig. 1 (or from Zorbax SB (no.18) to Zorbax Rx (no.24)). Nucleosil AB (no.26), with such a large value of the *cis/trans* separation factor, is a polyfunctional phase.

It can be noticed that the polymer-coated alumina phase (Gammabond C18, No.27) displays a *cis/trans* separation factor smaller than 1, indicating an inversion of the retention of the isomers, compared to the other phases.

Considering both separation factors on this diagram, it is possible to group the stationary phases having close properties. For instance: Kromasil C18 (no.23) and Zorbax Extend (no.25); or XTerra MS (no.20) and Uptisphere ODB (no.21). Moreover, as described in Fig. 1 through the bubble size, the hydrophobicity of Kromasil C18 and Zorbax Extend is close, while the XTerra MS is less retentive than Uptisphere ODB.

Based only on the accessibility to residual silanols evaluated by the separation of β-carotene and zeaxanthin, numerous phases would belong to the same group: non-endcapped phases Uptisphere NEC (no.1), Nucleosil 50 (no.2) and Nucleosil 100 (no.3); hydrophilic endcapped phases Aquasil (no.6), Prevail C18 (no.7); polar-embedded phases Polaris Ether (no.7), Symmetry Shield (no.9), Suplex pK_b (no.10), Supelcosil LC-ABZ (no.11), Supelcosil ABZ$^+$-Plus (no.12), Zorbax Bonus RP (no.14), Acclaim PA (no.15), Prevail amide (no.16) and Stability BS C23 (no.17); and "polar" phases, which exact nature is unknown to us: Platinum EPS (no.4), Polaris B (no.8) and Nucleosil Nautilus (no.13).

Judging by this observation, the phases having a "polar treatment", be it an embedded polar group or a polar endcapping group, seem to belong to the same group. In an aqueous mobile phase, these polar groups interact more or less with water. In the subcritical fluid used here, as would also be the case with a non aqueous liquid mobile phase, the polar groups are free to establish hydrogen bonds with zeaxanthin, inducing a large increase in the retention of this compound, that can even be more retained than β-carotene, thereby leading to a separation factor smaller than 1. In these analytical conditions, the behavior of these phases is similar to that of non-endcapped classical ODS phases.

The characterization through the carotenoid test thus leads to two possible confusions:

(1) Based on a β-carotene/zeaxanthin separation factor inferior to 1, it is impossible to discriminate a hydrophilic endcapping (nos. 5 and 6) from the phases possessing an amide-embedded group (nos. 11, 12, 14 and 16), or the low-coverage bonding of Platinum EPS (no.4), or the quaternary ammonium embedded of Stability BS C23 (no.17).
(2) Based on a β-carotene/zeaxanthin separation factor superior to 1, it is not possible to distinguish the non-endcapped phases (nos. 1, 2 and 3) and some polar-embedded phases (nos. 7, 9 and 15).

Some additional discrimination can be done if one considers the hydrophobic character evaluated by the retention factor of *all-trans*-β-carotene. This is represented on Fig. 1 through the size of the bubbles. Thus, for instance, a hydrophilic endcapping group (columns No.5 and 6) can be discriminated from an amide-embedded group (columns No.11, 12, 14 and 16) as the former is more hydrophobic than the latter, as reported elsewhere, since other authors have pointed out the low hydrophobicity of polar-embedded phases [41,42]. However, the distinction between the non-endcapped phases and the polar-embedded ones is still unclear as the hydrophobic character of the non-endcapped phases vary greatly among the three columns tested.

Thus, we have chosen 29 test-compounds and measured their retention factors on all the columns. The chosen compounds reflect a wide variety of interactive capabilities but are also smaller molecules than the carotenoid pigments and thus, they might interact more closely with the polar groups, polar endcapping groups and residual silanol groups than the carotenoid pigments.

3.2. κ–κ plots

First of all, the columns can be simply compared, based on the retention factors of the small probes, by plotting the retention factors measured on one column against the retention factors measured on a column chosen as a reference (so-called κ–κ plots). Kromasil C18 (no.23) was chosen as reference column (high bonding density, low silanol accessibility, high hydropho-

Please cite this article in press as: E. Lesellier, C. West, J. Chromatogr. A (2007), doi:10.1016/j.chroma.2007.03.072

bicity). When κ–κ plots of the retention data measured on different columns in the same analytical conditions are linear with unit slope, the retention behaviors are called homoenergetic [43] because of the similar physico-chemical interactions in the two chromatographic systems. Compounds not falling on a straight line indicate that the specific interactions are different.

Three general patterns can be observed.

In the first case (Fig. 2a), as is the case between Zorbax Rx (no.24) and Kromasil C18, the retention factors measured on the two columns are linearly correlated. Some slight dispersion can be noticed for acidic compounds (white diamonds), essentially due to very low retention of these solutes leading to less precise measurements. Aniline (white square) is also seen to be slightly more retained on Zorbax Rx, possibly due to interactions with residual silanol groups, as the carotenoid test indicated that Zorbax Rx is a little less protected against silanophilic interactions than Kromasil C18. Globally, Zorbax Rx and Kromasil C18 can be called homoenergetic. This is also the case with Zorbax SB (no.18), Zorbax Eclipse XDB (no.19), XTerra MS (no.20), Uptisphere ODB (no.21), Chromolith (no.22), Zorbax Extend (no.25) and Nucleosil AB (no.26).

In the second case (Fig. 2b), as is the case between Nucleosil 50 (no.2) and Kromasil C18 (no.23), two general trends can be noticed: non acidic and non basic compounds (black diamonds) are globally falling on a straight line, while acidic compounds (white diamonds) also fall on a straight line but with a different slope, as these solutes are more retained on Nucleosil 50 than on Kromasil C18. The *N*-containing basic solutes (white squares) do not fit in any of these regression lines, probably establishing some kind of electrostatic interactions, as explained in the experimental part. The columns are obviously not homoenergetic. This general pattern is also seen for Uptisphere NEC (no.1), Nucleosil 100 (no.3), Platinum EPS (no.4), Aquasil (no.5) and Prevail (no.6).

Finally, in the third case (Fig. 2c), as between Supelcosil ABZ$^+$-Plus (no.12) and Kromasil C18, acidic solutes (white diamonds) and non acidic solutes (black diamonds) again follow different trends, but, in this case, the basic solutes (white squares) fit well in the regression lines: aniline behaves as an acidic solute while *N*,*N*-dimethylaniline behaves as a non-acidic solute. Thus, no particular electrostatic interactions occur, but the acidic solutes are a lot more retained on Supelcosil ABZ$^+$-Plus than on Kromasil C18, thanks to its amide embedded group. This general pattern is also seen for Gammabond (no.27), Polaris Ether (no.7), Polaris B (no.8), Symmetry Shield (no.9), Suplex pK_b (no.10), Supelcosil LC–ABZ (no.11), Nucleosil Nautilus (no.13), Zorbax Bonus RP (no.14), Acclaim PA (no.15), Prevail Amide (no.16) and Stability BS C23 (no.17). The latter also shows a deviation of benzoic acid and isophthalic acid, possibly due to electrostatic interactions (see the experimental part).

Judging by the nature of this phase, the position of Gammabond in this latter group is somewhat surprising but we have not found any satisfying explanation to these results.

Thus, three groups can be defined, based on the relative interactions with acidic and basic solutes: columns no.18–26 (classical endcapped and classical with varied protection modes against silanophilic interactions); no.1–6 (classical non-

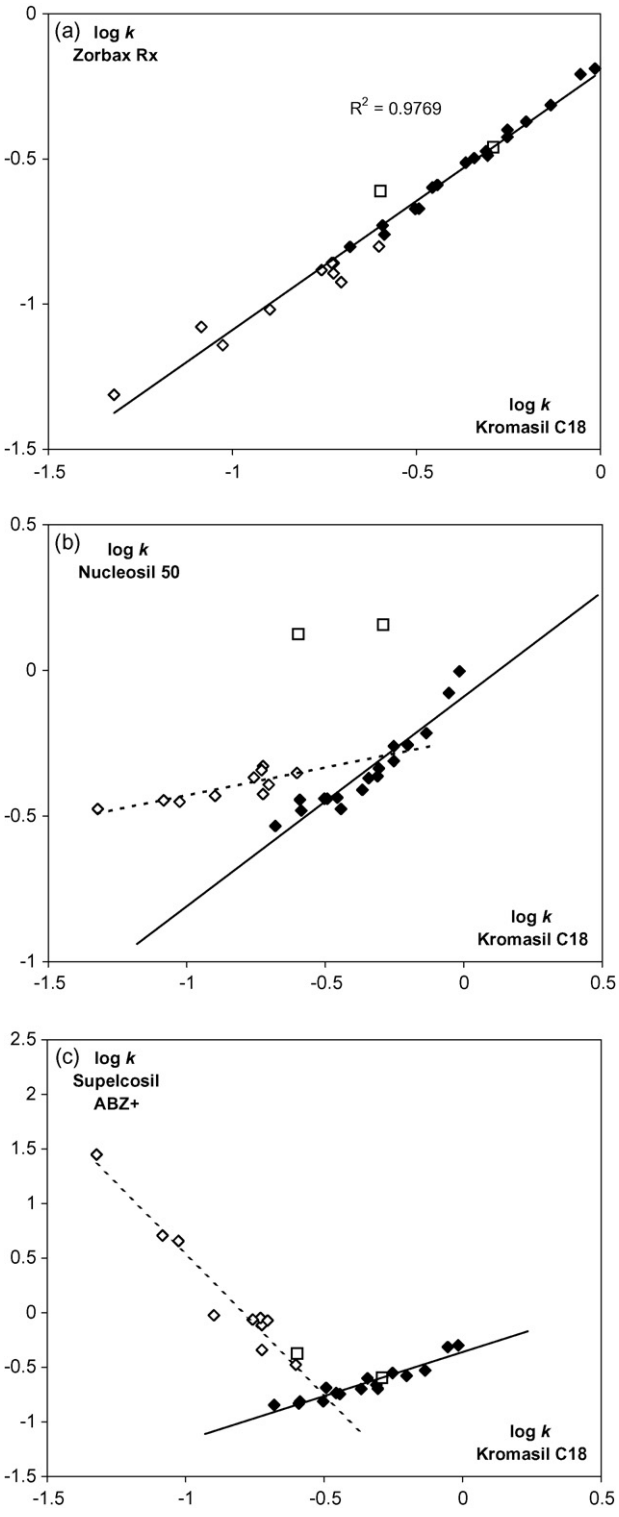

Fig. 2. (a) Plot of log *k* on Zorbax Rx vs. log *k* on Kromasil C18. (b) Plot of log *k* on Nucleosil 50 vs. log *k* on Kromasil C18. (c) Plot of log *k* on Supelcosil ABZ$^+$-Plus vs. log *k* on Kromasil C18. The solutes used are solutes 1–29 in Table 2. White diamonds are acidic compounds (all compounds having A > 0, Nos. 18–27); white squares are *N*-containing basic solutes (Nos. 28–29); black diamonds are all other solutes (nos.1–17). Chromatographic conditions: CO_2–MeOH 90:10 (v/v), 3 mL min^{-1}, outlet pressure 150 bar, temperature 25 °C.

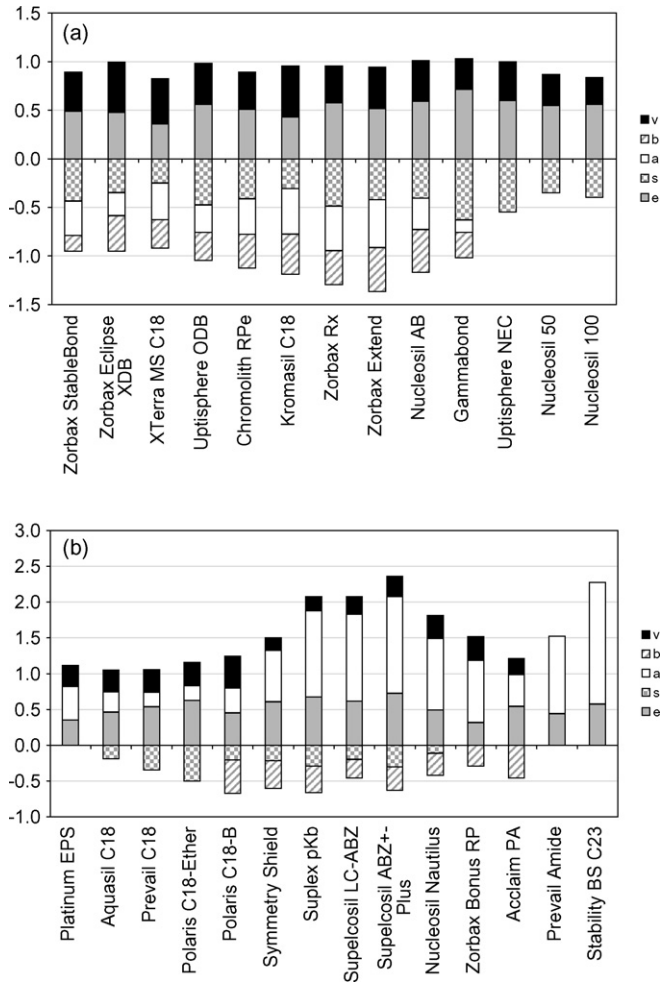

Fig. 3. Solvation parameter model coefficients compared for (a) classical ODS phases (b) ODS phases with hydrophilic endcapping and polar-embedded groups. Chromatographic conditions as in Fig. 2.

endcapped and hydrophilic endcapping groups); and no.7–17 (polar-embedded phases), plus no.27 (polymer coated alumina).

3.3. Solvation parameter model

Then quantitative structure–retention relationships (QSRR) were established, according to Eq. (1), between the retention factors of the 29 chosen probe solutes and their Abraham's descriptors E, S, A, B and V, to determine the e, s, a, b and v coefficients, indicating the strength of the interactions between the solutes and the stationary and mobile phases: charge transfer (e), dipole–dipole (s), hydrogen-bonding (a and b) and dispersion (v). The results are presented in Table 3 and Fig. 3.

Fig. 3a represents the values of the coefficients of the solvation parameter model for classical non-endcapped, endcapped and "protected" ODS phases. All columns display positive e and v coefficients, indicating that an increase in volume and in the polarisability of the solute induces an increase in retention on these phases. These terms are both related to dispersive interactions as an increase in volume and in polarizability both favor high dispersive interactions with the octadecyl chains.

Ten columns (Gammabond no.27, Nucleosil AB no. 26, Zorbax Extend no.25, Zorbax RX no.24, Kromasil no.23, Chromolith RP 18e no.22, Uptisphere ODB no.21, XTerra MS no.20, Eclipse XDB no.19 and Zorbax SB no.18) also display negative s, a and b coefficients, indicating that polar, acidic and basic solutes have greater interactions with the mobile phase than with the stationary phase thus are less retained on these stationary phases. However, Gammabond (no.27) seems to establish more interactions with acidic solutes than the other nine columns, as the negative a coefficient is larger (-0.128) on that column. This is consistent with previous observations based on the κ–κ plots.

For the non-endcapped columns Uptisphere NEC (no.1), Nucleosil 50 (no.2) and Nucleosil 100 (no.3), the a and b coefficients were found statistically not significant, indicating stronger interactions with acidic and basic solutes on these phases than on the previous ones. This clearly differentiates these phases from the endcapped and "protected" ones and corresponds to the classification based on the carotenoid test.

Fig. 3b displays the results obtained for phases possessing hydrophilic end-capping groups and polar embedded groups. The comparison of the histograms shows that none of these phases displays a similar behavior to that of classical endcapped and non-endcapped phases of Fig. 3a. It appears that the solvation parameter model allows a clear discrimination of polar embedded, end-capped phases and non end-capped C18 ones, while the carotenoid test was inefficient.

Contrary to the first group of columns (Fig. 3a), all these phases exhibit a positive a coefficient, indicating that all the "polar" treatments lead to increased retention – of varied magnitude – for acidic solutes. All phases from columns no. 9–17 possessing a nitrogen atom in their bonded chain (carbamate-, urea-, amide-, sulphonamide- and quaternary ammonium-embedded groups) display particularly strong interactions with acidic solutes (large a coefficients). The increased retention of acidic solutes on polar-embedded and polar-endcapped phases had already been mentioned by other authors [41,42,44]. Some of them [41] postulated that the enhanced retention of H-bond donors may be attributed to interaction of the solute with the highly polarized carbonyl oxygen of the polar embedded amide, urea, carbamate and sulphonamide groups. In comparison, the ether-based polar-embedded phase (Polaris Ether, no.7) does not exhibit such selectivity. Stability BS C23 (no.17), with its quaternary ammonium-embedded group, is the most basic of all phases studied here (a is equal to 1.702).

Judging by the size and magnitude of the coefficients, different groups can be defined (Fig. 3b):

(1) Platinum EPS (no.4) is different from all other columns.
(2) Aquasil (no.5), Prevail (no.6) and Polaris Ether (no.7) seem similar, if we except the fact that the latter does apparently not establish electrostatic interactions with possibly ionized basic solutes as the former two do (see experimental part).
(3) Polaris B (no.8) seems to be intermediate between hydrophilic end-capped and polar-embedded phases.
(4) Polar-embedded columns from no. 9 to 14 display a large basic character (large value of the a coefficient). This is due to the presence of a basic polar group embedded in the

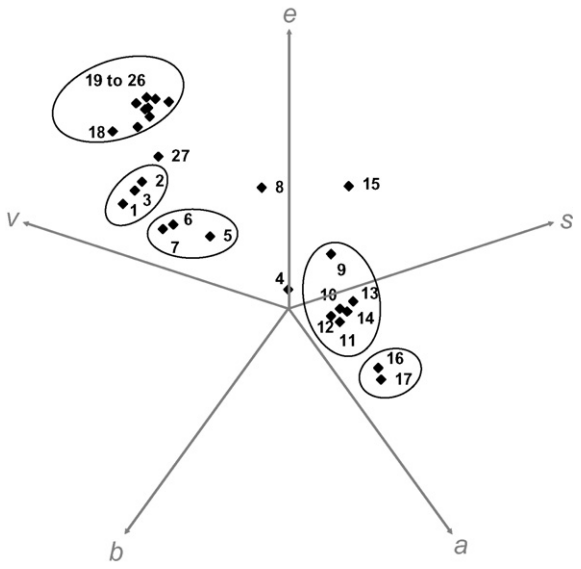

Fig. 4. "Spider" diagram for a five-dimensional representation of stationary phases evaluated with the solvation parameter model (Eq. (1)). Chromatographic conditions as in Fig. 2. Columns are numbered according to Table 1.

alkyl chain. The carbamate group of Symmetry Shield (no.9) seems a little less basic than the urea and amide groups of the other columns, since the *a* coefficient is a little smaller for that column.

(5) Acclaim PA (no.15), possessing a sulphonamide-embedded group is a little less basic than the preceding phases.

(6) Prevail Amide and Stability BS C23 seems similar. These are the only columns where the volume of the solute, *i.e.* the dispersive interactions, has no influence on retention.

As it is still complicated to compare so many columns based on five interaction terms, the results were plotted on a "spider" diagram (Fig. 4), providing a representation in the five-dimensional space [3]. On this diagram, columns located in the same area display close selectivity. Furthermore, the groups evidenced on this figure are based on the calculation of the *J* factor, based on Eqs. (4)–(6). Thus, all columns circled are considered to be similar at the 99% confidence level.

Thus, based on the solvation parameter model, five groups can be established, along with four columns not belonging to any group:

(1) the classical, endcapped or protected ODS are grouped together (nos.18–26).

(2) The classical non-endcapped columns are grouped together (columns no.1–3).

(3) The phases with a hydrophilic end-capping (Aquasil no.5 and Prevail no.6) and the only polar-embedded phase that does not contain any nitrogen atom (Polaris Ether no.7) are grouped together. Additionally, polar-end-capped columns more closely resemble type-B classical columns than polar-embedded columns, a fact that was also mentioned by other authors [42].

(4) Apart from Prevail Amide (no.16), that is surprisingly different from them, all amide-embedded phases are grouped together (Nos.11, 12 and 14) along, with the carbamate-embedded phase (no.9), the urea-embedded phase (no.10) and with Nucleosil Nautilus (no.13), which exact identity is unknown to us.

(5) Prevail Amide (no.16) and Stability BS C23 (no.17) are grouped together. This is quite surprising as Prevail Amide is not known to have any ammonium group in its bonding structure.

Gammabond (no.27), Polaris B (no.8), Platinum EPS (no.4) and Acclaim PA (no.15) are unique and do not belong to any group. Among these phases, Gammabond is known to be prepared on alumina and coated by a polymer while all other phases are prepared on silica, which could explain its difference. The exact nature of Polaris B and Platinum EPS is unknown to us but the former is possibly some sort of polar-embedded phase (probably not *N*-containing), while the latter is simply known to have an intentionally low bonding density (about 5% carbon content). Other authors already reported that the structure of Polaris phases lead to unusual behaviors [41]. Acclaim PA is the only column to have a sulphonamide-embedded group.

Thus, the different bonding chemistries of the polar-embedded phases are well discriminated by the solvation parameter model used in subcritical fluid conditions, and only carbamate and urea are not clearly discriminated from amide groups.

3.4. Combination of the large and small probes

3.4.1. Principal component analysis

The two different testing procedures presented here (carotenoid test and solvation parameter model) are seen to provide somewhat different results. To get a global comparison of all columns tested here, the results issued from both tests were combined. First of all, a principal component analysis (PCA) was performed on the retention and separation factors of the carotenoid probes, together with the coefficients issued from the solvation parameter model. As the solvation parameter coefficients are related to the logarithm of the retention factors, the results of the carotenoid test were also converted to their logarithmic form.

In PCA, the number of variables (in this case, the eight column parameters, three issued from the carotenoid test and five from the solvation parameter model) is reduced onto a smaller number of new variables called principal components (PC). The score plots representing the projection of the objects (in this case, the columns) onto the PCs allows a graphical estimation of similarities between the objects, while the loading plot representing the contribution of the original variables (in this case, the column parameters) to the principal components allows to see which variables are the most important and if any of them are correlated.

The first four principal components explain less than 90% of the variance, with PC1 and PC2 together explaining 61% of the variance, PC3 and PC4 explaining 27% of the variance. Conse-

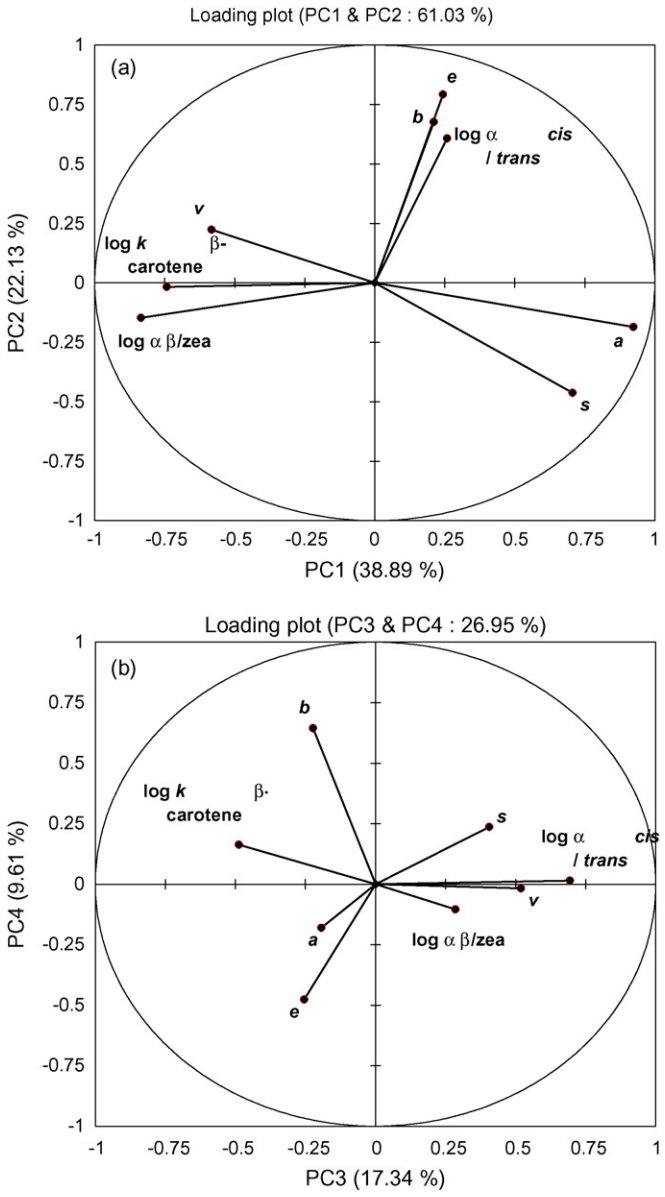

Fig. 5. Loading plots of (a) PC1–PC2 and (b) PC3–PC4 obtained for a principal component analysis based on the three separation and retention factors of the carotenoid test and the five coefficients issued from the solvation parameter model analysis, for the 27 columns characterized.

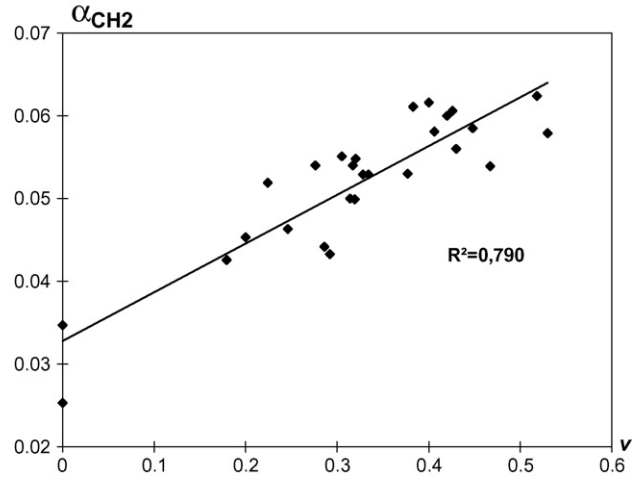

Fig. 6. Plot of the methylene selectivity (based on the retention factors of alkylbenzenes from C2 to C5) *vs.* the *v* coefficient of the solvation parameter model. Chromatographic conditions as in Fig. 2.

quently, no clear trends can be drawn from the score plots as the information is parted in two. However, the loading plots (Fig. 5) are interesting because they indicate that the three criteria of the carotenoid test and the five criteria of the solvation parameter model are not correlated. Indeed, all the factors that seem to be correlated on the PC1–PC2 plane (Fig. 5a), standing for 61% of the variance, are not correlated on the PC3–PC4 plane (Fig. 5b), standing for 27% of the variance.

For instance, if the separation factor between the 13-*cis* and *all-trans* isomers of β-carotene seems to be correlated to the *e* and *b* coefficients on PC1–PC2, it is not at all the case on PC3–PC4. This is not surprising since the shape recognition evaluated by the separation factor between 13-*cis*- and *all-trans*-β-carotene is largely related to a geometrical factor, independent of any differences in the physico-chemical properties of the solutes evaluated by the solvation parameter model. Thus, shape recognition cannot be evaluated by the small probes as it was evaluated by the carotenoid probes.

Besides, the retention factor of the *all-trans*-β-carotene, evaluating the hydrophobic character of the stationary phase, is not correlated to the *v* coefficient, associated to dispersive interactions: the correlation coefficient between them is only 0.29. This is not surprising as the hydrophobicity evaluated by the carotenoid probe is determined by surface area, carbon load, ligand chain length, bonding chemistry and end-capping treatments [2], while in the solvation parameter model, the coefficient mainly related to surface area is the regression intercept *c*, which we have not discussed of as it may also contain all information not included in the model coefficients. Indeed, the regression intercept *c* and the retention factor of the *all-trans*-β-carotene show some degree of correlation ($R^2 = 0.62$). The *v* coefficient, on the other hand, is mostly related to methylene selectivity, as can be seen on Fig. 6. However, methylene selectivity is known to be inappropriate to estimate the hydrophobicity of a stationary phase [24]. Thus, there is no reason why the retention of *all-trans*-β-carotene and the *v* coefficient should be related and they really provide complementary information.

Finally, although it is not obvious on the loading plots, the logarithm of the separation factor between *all-trans*-β-carotene and zeaxanthin is inversely correlated to the *a* coefficient. Indeed, when they are plotted one against the other, there is a linear trend between these two factors ($R^2 = 0.690$), with a negative slope: the stationary phases displaying a negative *a* coefficient, therefore establishing only small interactions with acidic solutes, also show large values of the *all-trans*-β-carotene/zeaxanthin separation factor, while the phases displaying a positive value of the *a* coefficient, therefore strong interactions with acidic solutes, have only small values of the *all-trans*-β-carotene/zeaxanthin separation factor. Thus, in the interaction established between zeaxanthin and the stationary phase, zeaxanthin mostly behaves as a hydrogen-donating solute.

Please cite this article in press as: E. Lesellier, C. West, J. Chromatogr. A (2007), doi:10.1016/j.chroma.2007.03.072

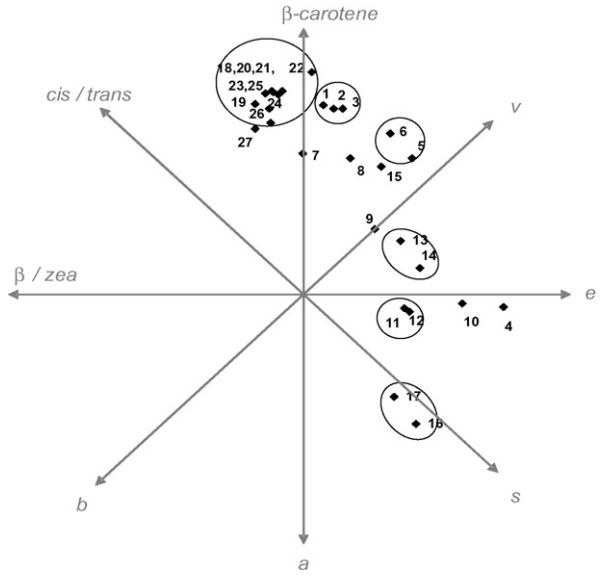

Fig. 7. "Spider" diagram for a eight-dimensional representation of stationary phases evaluated with both the solvation parameter model (Eq. (1)) and the carotenoid test. Chromatographic conditions as in Figs. 1 and 2. Columns are numbered according to Table 1.

A better correlation can be found if one also considers the *b* coefficient, judging that zeaxanthin can also behave as a hydrogen-bond accepting solute. Indeed, a multiple linear regression of the logarithm of the *all-trans*-β-carotene/zeaxanthin separation factor on the *a* and *b* coefficients leads to a good correlation ($R^2 = 0.887$), with the two coefficients (*a* and *b*) both negatively and significantly contributing to the dependent variable ($\log \alpha_{\textit{all-trans}\text{-β-carotene/zeaxanthin}}$).

This would tend to indicate that, to estimate hydrogen bond interactions, the results based on solutes with very different sizes can be well correlated. This is particularly interesting as there is a major concern that column characteristics obtained from small molecules do not necessarily provide the required information for a proper selection of columns for the separation of larger molecules, while the results presented here would tend to show the contrary.

Besides, this also indicates that seven factors could be enough for a classification of the columns as the *all-trans*-β-carotene/zeaxanthin separation factor can be advantageously replaced by the *a* and *b* coefficients.

However, judging by the complexity of the problem, the eight factors are all necessary and cannot be reduced down to two dimensions. Thus, some other way of combining the data is required to get a clear global view of the column classification.

3.4.2. Comparison based on the solvation vectors

The θ_{ij} angles existing between the solvation vectors associated to all the stationary phases characterized above through the use of both the solvation parameter model and the carotenoid test were calculated according to Eq. (3b). Then the *J* similarity factor was calculated according to Eqs. (4)–(6). Thus, the couples of stationary phases that were judged to be similar at the 99% confidence level are represented on Fig. 7. This last figure is constructed using the same principles as Fig. 4, but considering the eight criteria. The axes were placed in such a manner that the most correlated factors are positioned close to each other.

The addition of three more criteria, compared to Fig. 4, produces a finer classification.

Columns 9–14 that were all in the same group on Fig. 4 are now separated in four groups: Symmetry Shield (no.9), the only carbamate-embedded phase is separated from the amide-embedded phases, the urea-embedded Suplex pK_b (no.10) is also separated from the others, while Supelcosil LC–ABZ and Supelcosil ABZ$^+$Plus on the one hand (nos.11 and 12), Nucleosil Nautilus and Zorbax Bonus RP (nos.13 and 14) on the other hand remain grouped together.

Besides, Polaris C18-Ether (no.7) is now clearly separated from the hydrophilic-end-capped phases (nos.5 and 6).

Gammabond (no.27), although displaying a small angle with all classical columns, is judged different from them according to the calculation of the *J* factor.

4. Conclusion

The characterization of ODS phases with the solvation parameter model offers a fine complement to the results obtained with the carotenoid test, particularly for the discrimination of polar-embedded phases from non-end-capped ODS phases. Moreover, this approach allows a finer discrimination of polar-embedded phases, depending on the nature of the embedded polar group, and of certain unspecified phases.

A classification of the phases according to an increasing basic character (*a* coefficient) would be the following: end-capped classical ODS phases < non-end-capped classical ODS phases < hydrophilic end-capping groups < ether-embedded phases < carbamate-embedded phases < amide- and urea-embedded phases < ammonium-embedded phases.

The data treatments and presentation of the results based on a 5- or 8-axes spider diagram allows the visualization of all phases on a unique figure, and an easy comparison. Moreover, the similarities are defined on the basis of an objective calculated factor (*J*).

Correlations have been found between the methylene selectivity and the *v* coefficient and between the β-carotene/zeaxanthin separation factor and the *a* and *b* coefficients.

Acknowledgment

We wish to thank the manufacturers who kindly provided the stationary phases for this study.

References

[1] U.D. Neue, K. Van Tran, P. Iraneta, B.A. Alden, J. Sep. Sci. 26 (2003) 174.
[2] H.A. Claessens, M.A. Van Straten, C.A. Cramers, M. Jezierska, B. Buszewski, J. Chromatogr. A 826 (1998) 135.
[3] C. West, E. Lesellier, J. Chromatogr. A 1110 (2006) 191.
[4] M.H. Abraham, A. Ibrahim, A.M. Zissimos, J. Chromatogr. A 1037 (2004) 29.
[5] C.F. Poole, S.K. Poole, J. Chromatogr. A 965 (2002) 263.
[6] L.C. Tan, P.W. Carr, M.H. Abraham, J. Chromatogr. A 752 (1996) 1.
[7] L.C. Tan, P.W. Carr, M.H. Abraham, J. Chromatogr. A 799 (1998) 1.

[8] A. Sandi, L. Szepesy, J. Chromatogr. A 818 (1998) 1.
[9] A. Sandi, L. Szepesy, J. Chromatogr. A 818 (1998) 19.
[10] A. Sandi, L. Szepesy, J. Chromatogr. A 893 (2000) 215.
[11] M. Reta, P.W. Carr, P.C. Sadek, S.C. Rutan, Anal. Chem. 71 (1999) 3484.
[12] L. Szepesky, J. Sep. Sci. 26 (2003) 201.
[13] C. Lepont, A.D. Gunatillaka, C.F. Poole, Analyst 126 (2001) 1318.
[14] J.A. Blackwell, P.W. Carr, J. High Resolut. Chromatogr. 21 (1998) 427.
[15] D. Pyo, W. Li, M.L. Lee, J.D. Werkwerth, P.W. Carr, J. Chromatogr. A 753 (1996) 291.
[16] D. Pyo, H. Kim, J.H. Park, J. Chromatogr. A 796 (1998) 347.
[17] J.A. Blackwell, R.W. Stringham, J. High Resolut. Chromatogr. 20 (1997) 631.
[18] C. West, E. Lesellier, A. Tchapla, J. Chromatogr. A 1048 (2004) 99.
[19] C. West, E. Lesellier, J. Chromatogr. A 1087 (2005) 64.
[20] C. West, E. Lesellier, J. Chromatogr. A 1110 (2006) 181.
[21] C. West, E. Lesellier, J. Chromatogr. A 1110 (2006) 200.
[22] C. West, E. Lesellier, J. Chromatogr. A 1115 (2006) 233.
[23] E. Lesellier, A.M. Krstulovic, A. Tchapla, J. Chromatogr. A 645 (1993) 29.
[24] E. Lesellier, A. Tchapla, J. Chromatogr. A 1100 (2005) 45.
[25] E. Lesellier, C. West, A. Tchapla, J. Chromatogr. A 1111 (2006) 62.
[26] L. Zeichmeister, P. Tuzson, Biochem. J. 32 (1938) 1305.
[27] J. Li, J. Chromatogr. A 982 (2002) 209.
[28] J. Li, Anal. Chim. Acta 522 (2004) 113.
[29] J. Li, J. sun, S. Cui, Z. He, J. Chromatogr. A 1132 (2006) 174.
[30] M. Rosés, D. Bolliet, C.F. Poole, J. Chromatogr. A 829 (1998) 29.
[31] M.H. Abraham, Y.H. Zhao, J. Org. Chem. 69 (2004) 4677.
[32] Y.H. Zhao, M.H. Abraham, A.M. Zissimos, J. Chem. Inf. Comput. Sci. 43 (2003) 1848.
[33] D. Wen, S.V. Olesik, Anal. Chem. 72 (2000) 475.
[34] K.L. Toews, R.M. Shroll, C.M. Wai, N.G. Smart, Anal. Chem. 67 (1995) 4040.
[35] J. Zheng, Supercritical fluid chromatography of ionic compounds, PhD thesis, Virginia Polytechnic Institute, Blacksburg, VI, 2005.
[36] Y. Ishihama, N. Asakawa, J. Pharm. Sci. 88 (1999) 1305.
[37] K. Kimata, K. Iwagushi, S. Onishi, K. Jinno, R. Eksteen, K. Hosoya, M. Araki, N. Tanaka, J. Chromatogr. Sci. 27 (1989) 721.
[38] U.D. Neue, E. Serovik, P. Iraneta, B.A. Alden, T.H. Walter, J. Chromatogr. A 849 (1999) 87.
[39] U.D. Neue, B.A. Alden, T.H. Walter, J. Chromatogr. A 849 (1999) 101.
[40] U.D. Neue, Y.F. Cheng, Z. Lu, B.A. Alden, P.C. Iraneta, C.H. Phoebe, K. Van Tran, Chromatographia 54 (2001) 169.
[41] M.R. Euerby, P. Petersson, J. Chromatogr. A 1088 (2005) 1.
[42] N.S. Wilson, J. Gilroy, J.W. Dolan, L.R. Snyder, J. Chromatogr. A 1026 (2004) 91.
[43] D. Corradini, K. Kalghatgi, C. Horváth, J. Chromatogr. A 728 (1996) 225.
[44] H. Engelhardt, R. Grüner, M. Scherer, Chromatographia 53S (2001) S154.

Please cite this article in press as: E. Lesellier, C. West, J. Chromatogr. A (2007), doi:10.1016/j.chroma.2007.03.072